Journal of
Applied Remote Sensing

Modification and validation of a quasi-analytical algorithm for inherent optical properties in the turbid waters of Poyang Lake, China

Jue Huang
Liqiong Chen
Xiaoling Chen
Liqiao Tian
Lian Feng
Hervé Yesou
Fangfang Li

Modification and validation of a quasi-analytical algorithm for inherent optical properties in the turbid waters of Poyang Lake, China

Jue Huang,[a] Liqiong Chen,[a] Xiaoling Chen,[a,*] Liqiao Tian,[a] Lian Feng,[a] Hervé Yesou,[b] and Fangfang Li[c]

[a]Wuhan University, State Key Laboratory of Information Engineering in Surveying, Mapping and Remote Sensing, 129 Luoyu Road, Wuhan 430079, China
[b]Université de Strasbourg, SERTIT, Bld Sébastien Brant, BP 10413, Illkirch 67412, France
[c]National University of Defense Technology, College of Information Systems and Management, Changsha 410073, China

Abstract. Knowing the inherent optical properties (IOPs) of water bodies is useful for many water environment studies and applications. To derive the IOPs from remote sensing reflectance, a multiband quasi-analytical algorithm (QAA) was modified and validated for the highly turbid Poyang Lake in China. In order to supplement and expand the dynamic variation range of the measured water optical properties, a Hydrolight simulated dataset was generated to develop a regional QAA (QAA710) for this area. The QAA710 model was then validated with simulated data, simulated data with random noise, and *in situ* data. The results show that the effects of random noise (within ±20%) of remote-sensing reflectance on the derived total absorption coefficients (a_t) and the particulate backscattering coefficients (b_{bp}) by the QAA710 model are insignificant (a band-averaged mean relative error of 4.1% and 12.0%, respectively). The validation of *in situ* a_t shows a 28.6% mean relative difference. The model process, modeling data, and validation data introduce uncertainties into the derived results. These analyses demonstrate that the QAA710 model, based on the characterization of local environments, performs well in retrieving Poyang Lake's IOPs. © *2014 Society of Photo-Optical Instrumentation Engineers (SPIE)* [DOI: 10.1117/1.JRS.8.083643]

Keywords: inherent optical properties; Poyang lake; quasi-analytical algorithm; radiative transfer model.

Paper 13500 received Dec. 2, 2013; revised manuscript received Mar. 25, 2014; accepted for publication Mar. 27, 2014; published online Apr. 28, 2014.

1 Introduction

The water inherent optical properties (IOPs) are crucial for remote sensing retrieval. IOPs consist of absorption and scattering coefficients of several natural constituents, such as phytoplankton, nonalga particles, and colored dissolved organic matter (CDOM). Unaffected by light irradiated into the water, IOPs only depend on the optical properties of water constituents. As a result, IOPs are widely used to retrieve the concentrations of water constituents from remote sensing imagery and to determine the turbidity and primary production.[1–3] Methods to accurately retrieve IOPs remotely have been under investigation for years, and algorithms from empirical to analytical algorithms have been proposed and validated.[4,5]

Limited by the nature of regression, the empirical algorithms are generally only appropriate to waters with characteristics similar to those used in the algorithm development. Their applicability can be quite limited and may result in significant errors.[6] In comparison, the semianalytical algorithms demonstrate better applicability and can obtain more information of water optical properties based on the solutions of radiative transfer equations. [7,8] Various semianalytical

*Address all correspondence to: Xiaoling Chen, E-mail: cxl@lmars.whu.edu.cn

algorithms for IOPs retrieval have been presented and intercompared with in the framework of the International Ocean Color Coordinating Group.[9] Certain algorithms, such as the Garver-Siegel-Maritorena (GSM) semianalytical bio-optical model[10] and the moderate-resolution imaging spectrometer semianalytical algorithm[11] are more suitable for retrieving IOPs in lower absorption situations. In contrast, the quasi-analytical algorithm (QAA) developed and revised by Lee et al.[6,12,13] is mathematically simple, physically transparent with better adaptability.[9]

Given an estimate of the spectral dependence of the absorption and scattering coefficients, the QAA model retrieves the total absorption coefficient $a_t(\lambda)$ and particulate backscattering coefficient $b_{bp}(\lambda)$ with relatively little *a priori* knowledge of the spectral slopes of water components. The default reference wavelength of the QAA algorithm is 555 nm for clear oceanic water, where $a_t(555)$ is dominated by pure water.[6] This reference wavelength should be shifted to a longer waveband in higher absorbing water because the absorption of suspended solids and gelbstoff makes considerable contributions to $a_t(555)$.[6,14] Studies have shown that after suitable modifications, the QAA model has good adaptability to coastal areas and inland lakes, such as the Yellow and East China Sea, the Monterey Bay, the Gulf of Mexico, the Arabian Sea, and China's Taihu Lake.[5,12,15,16]

Poyang Lake, the largest freshwater lake lying in Jiangxi Province, China, is far more turbid than these water bodies. High turbidity makes the lake one of the most difficult areas for developing remote sensing algorithms. Current studies primarily focus on analysis of *in situ* data and parameters retrieval with empirical algorithms.[17–19] As mentioned above, the applicability of empirical algorithms is limited by seasonal and spatial variation, so the semianalytical algorithm, QAA, may be a better choice for IOPs' retrieval in highly turbid Poyang Lake.

In addition, some optical instruments cannot get valid results because water optical properties of Poyang Lake are beyond their designing ranges. For example, in our 2011 cruise, the signals of BB9 (WET Labs, Philomath, Oregon) were saturated for most observation sites, leading to no valid *in situ* backscattering coefficients for validation in this research. Therefore, we try to generate a set of simulated data with the help of a forward radiative transfer model. These simulated data will make up for the deficiency of *in situ* data and validate semianalytical algorithm QAA.

The primary objective of this study is to modify and validate the QAA model in the highly dynamic and turbid water of Poyang Lake. The specific goals are: (1) to generate a simulated data set based on a forward radiative transfer model to supplement *in situ* data; (2) to improve the performance of the QAA model by switching the reference wavelength with parameter tuning; and (3) to validate the region-specific QAA algorithm with simulated data and *in situ* data. The results from this article provide an alternative approach to investigate IOPs variation in Poyang Lake.

2 Study Area and Data Sets

2.1 *Study Area*

Poyang Lake (28°24′ to 29°26′ N, 115°49′ to 116°46′ E) is the largest freshwater lake in China. It lies in northern Jiangxi Province near the south bank of middle and lower reaches of the Yangtze River (see Fig. 1). The lake receives its water from five main tributaries (Ganjiang, Fuhe, Xiushui, Raohe, and Xinjiang) and drains into the Yangtze River through a channel in the north.[20] Poyang Lake is characterized by a rapid change in the lake inundation area; its size fluctuates from less than 1000 km^2 in the dry season to larger than 3000 km^2 in the flood season.[19,21] In addition, Poyang Lake is much more turbid than comparable inland lakes and coastal waters.[5,15,22,23] An investigation cruise in July 2011 revealed that the average total-suspended matter (TSM) of Poyang Lake was 48.31 mg/l with a maximum value of 158.82 mg/l. As one of the most important tributary water systems of the Yangtze River, Poyang Lake plays an important role in bolstering local economic and social development, as well as ecological conservation.[24]

2.2 *In Situ Data*

Field measurements were conducted on July 15 to 23, 2011, during the flood season of Poyang Lake. The water optical properties, concentration of water constituents, and ancillary data were

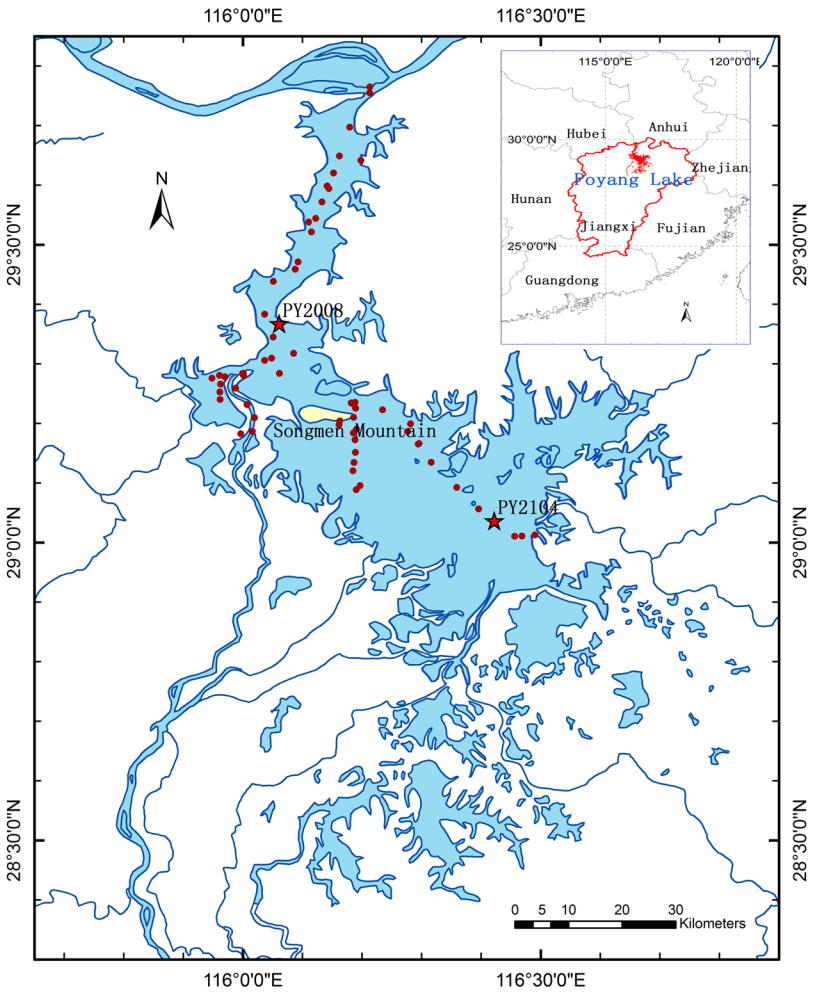

Fig. 1 Distribution of observation sites during the Poyang Lake cruise in July 2011. Two representative observation sites (PY2008 and PY2104) with different water qualities and geographical conditions are labeled with stars.

collected. The location of observation sites is shown in Fig. 1, and the measured parameters are listed in Table 1.

The remote sensing reflectance $R_{rs}(\lambda)$ was recorded with an HR-1024 field-portable spectrometer (Spectra Vista Corporation, New York) following NASA protocols for the above-water spectra measurement method. $R_{rs}(\lambda)$ (sr^{-1}) was calculated as follows:

$$R_{rs}(\lambda) = (L_w - rL_{sky})\rho_P/(L_P\pi), \quad (1)$$

Table 1 Statistics describing the particulate absorption coefficients at 443 nm [$a_p(443)$], concentrations of colored dissolved organic matter (CDOM), chlorophyll (Chl), and total-suspended matter (TSM) from the Poyang Lake cruise in July 2011.

	N[a]	Max	Min	Mean
$a_p(443)$ (m^{-1})	37	20.87	5.04	10.48
CDOM (m^{-1})[b]	61	2.74	0.36	0.89
Chl (μg/l)	61	12.89	0.50	4.25
TSM (mg/l)	61	158.82	3.192	48.31

[a]N represents the number of observation sites.
[b]CDOM is represented by the absorption coefficient of CDOM at 400 nm, $a_g(400)$.

where L_w, L_{sky}, and L_p were the radiances of the water, sky, and the reference plank, respectively; and r was the coefficient of Fresnel reflection ($r \approx 0.025$ when the wind speed is 5 m/s) and ρ_p was the known reflectance of the reference plank.

Water samples were filtered through 0.7-μm Whatman (Maidstone, United Kingdom) GF/F filters of 47-mm diameter. The $a_p(\lambda)$ was measured by UV-2550 UV-VIS spectroscopy (Shimadzu, Kyoto, Japan) using the transmittance technique.[25] After bleaching with NaClO (0.1%), the nonalga particle absorption $a_{NAP}(\lambda)$ was similarly recorded. Then, the absorption coefficient of phytoplankton $a_{ph}(\lambda)$ was calculated in Eq. (2).[25]

$$a_{ph}(\lambda) = a_p(\lambda) - a_{NAP}(\lambda). \tag{2}$$

The water samples for CDOM were first filtered through a 0.22-μm Millipore (Darmstadt, Germany) filter and kept in liquid nitrogen away from light. Then, the absorption of CDOM was measured using a liquid waveguide capillary cell (LWCC) measurement system, consisting of an Ocean Optical HR2000 spectrometer (Ocean Optics, Dunedin, New Zealand), a light source and a LWCC with a 1-m optical path. The absorption spectra of filtered water between 350 and 800 nm were recorded by the HR2000 spectrometer, when the water was flowing through the LWCC. Designating pure water as a baseline, absorption coefficient of CDOM $a_g(\lambda)$ was calculated by fitting the spectra in Eq. (3):[25]

$$a_g(\lambda) = a_g(\lambda_0) \times e^{[-S(\lambda-\lambda_0)]} + K, \tag{3}$$

where S represented the spectral slope of CDOM and K represented the mean value of the $a_g(\lambda)$ between 700 and 800 nm.

Following the gravimetric method,[15] water samples were filtered through dried and preweighed 0.45-μm Whatman polycarbonate membranes. The TSM was obtained by reweighing the samples after they had been dried at 45°C for 24 h until the difference of successive calculated TSM was <0.01 mg/l.

Chlorophyll-a standards purchased from Sigma Chemical Co., St. Louis, Missouri were used to calibrate the fluorescent spectrophotometer before the experiment. Then, chlorophyll samples were filtered through 0.45-μm Whatman cellulose acetate membranes and stored in liquid nitrogen immediately after filtration. The filters were soaked with ethanol (90%) at 0°C for 24 h for extraction. After that, the concentration of chlorophyll (Chl) was determined by measuring the extracted pigment samples using a RF-5301 fluorescent spectrophotometer (Shimadzu, Kyoto, Japan). The exciting wavelength and fluorescent wavelength were 432 and 667 nm, respectively.

3 Methodologies

3.1 *Data Simulation with Hydrolight Radiative Transfer Model*

The Hydrolight model solves the radiative transfer equation using a numerical technique. It computes the radiance distribution of the water environment based on the IOPs and appropriate boundary conditions at the surface and bottom of water body.[26] This model is widely used in water remote sensing research and is undergoing continuous debugging and validation.[27] With the help of the Hydrolight model, we used the forward calculations to generate a population of synthetic samples. These simulated data supplemented and expanded the dynamic variation range of the water optical properties of Poyang Lake.

The IOPs of natural water are usually defined as the function of absorption and scattering coefficients of different water constituents.

$$a_t(\lambda) = a_w(\lambda) + a_{ph}(\lambda) + a_{NAP}(\lambda) + a_g(\lambda), \tag{4}$$

$$a_{ph}(\lambda) = \mathrm{Chl} \times a^*_{ph}(\lambda), \tag{5}$$

$$a_{NAP}(\lambda) = \mathrm{TSM} \times a^*_{NAP}(\lambda). \tag{6}$$

As described in Eq. (4), the total absorption coefficient $a_t(\lambda)$ was the sum of the absorption coefficients of pure water $a_w(\lambda)$,[28] phytoplankton $a_{ph}(\lambda)$, CDOM $a_g(\lambda)$, and nonalga particles $a_{NAP}(\lambda)$.[29] Concerning Eqs. (5) and (6), the $a_{ph}(\lambda)$ and $a_{NAP}(\lambda)$ were defined by the specific absorption coefficients of phytoplankton $a^*_{ph}(\lambda)$ and nonalga particles $a^*_{NAP}(\lambda)$,[30] respectively, whose spectra were determined by the *in situ* data of Poyang Lake. The $a_g(\lambda)$ decreases exponentially with wavelengths [Eq. (3)] and the spectral slope was estimated to be 0.0142 nm^{-1} according to field measured data.

$$b_b(\lambda) = b_{bw}(\lambda) + b_{bph}(\lambda) + b_{bNAP}(\lambda), \tag{7}$$

$$b_b(\lambda) = b_{bw}(\lambda) + (b_b/b)_{ph} \times b_{ph}(\lambda) + (b_b/b)_{NAP} \times b_{NAP}(\lambda). \tag{8}$$

The total backscattering coefficient $b_b(\lambda)$ was the sum of the backscattering coefficient of pure water $b_{bw}(\lambda)$, phytoplankton $b_{bph}(\lambda)$, and nonalga particles $b_{bNAP}(\lambda)$ in Eq. (7). Because of the lack of *in situ* data, the specific scattering coefficients embedded in the Hydrolight software were applied to the simulation. Thus, Eq. (7) can be rewritten as Eq. (8). According to our observation, the extremely high turbidity of Poyang Lake made the transparency of most observation sites <30 cm, leading to optical deep water. Therefore, we assumed that the stratification effect and bottom effect were negligible.

To supplement and expand the dynamic variation range of the measured water optical properties, the concentrations of water constituents varied within and beyond their measured ranges at Poyang Lake in the simulation (see Table 2).

3.2 *QAA710 Model and mQAA640 Model*

The Hydrolight radiative transfer model produced 850 sets of simulated spectra. One third of the spectra (255 sets) served as random samples for validation, and the remainders (595 sets) were used for model construction.

The QAA model is first developed by Lee et al.[6] and has been revised several times.[12,13] Based on an empirical inversion equation at a reference wavelength, the QAA propagates the calculation of IOPs to other wavelengths under the assumption that $b_{bp}(\lambda)$ varies in a power-law function of wavelength. Little *a priori* knowledge of the water components spectral slopes is required for calculating $a_t(\lambda)$ and $b_{bp}(\lambda)$.

Table 2 Input parameters for Hydrolight simulation.

Variables	Inputs						
Sun zenith angle	30 deg						
Wind speed	5 m/s						
Water depth	Indefinite						
Wavelength	410 to 750 nm, every 10 nm						
Particle phase function	$(b_b/b)_{ph}$ 0.015; $(b_b/b)_{NAP}$ 0.025 (Refs. 31–33)						
Chl (μg/l)	0.5	1.0	1.5	2.0	3.0	5.0	8.0
	10.0	15.0	20.0				
CDOM (m^{-1})	0.5	0.8	1.1	1.5	2.0		
TSM (mg/l)	1.0	2.0	5.0	10.0	15.0	20.0	25.0
	30.0	40.0	50.0	60.0	80.0	100.0	150.0
	200.0	250.0	300.0				

Originally designed for ocean water, the empirical parameters of the QAA model should be tuned to accommodate the water optical properties of inland lakes.[15] Therefore, we built new equations of a_t and r_{rs} ratios with the regional simulated data set. First, the reference wavelength should be shifted to a longer waveband. As described in Fig. 2 of Lee et al.,[6] for clear oceanic water the absorption of pigment and particles at 555 nm or longer wavelengths is quite small, with a_t dominated by the values of a_w. So, the 555 nm is chosen as the reference wavelength. But, this is not the case in highly turbid waters because absorption at 555 or 640 nm is dominated by suspended solids. As a result, 710 nm may be a more appropriate choice.[14,15] Figure 2 presents examples of a_t variations in highly turbid Poyang Lake. In these examples, a 4-fold $a_t(640)$ variation corresponds to a factor of two variation for $a_t(710)$ and just a fractional variation for $a_t(800)$. These facts suggest that, a_t can be well estimated around 710 nm. Second, the wavelength located near the center of a satellite channel was given top priority with the expectation that the modified QAA model would be applied to satellite images such as the medium resolution imaging spectrometer (MERIS). Taking all these factors into consideration, 710 nm (near the center of MERIS channel 9) was chosen as the reference wavelength. According to the measured data of Poyang Lake, $r_{rs}(710)$ can be accurately measured. $r_{rs}(560)$ is insensitive to the variation of suspended particles and locates at the center of MERIS channel 5. So, the wavelength ratio $r_{rs}(710)/r_{rs}(560)$ may be a good proxy for a_t. In addition, there is a good correlation between the total absorption coefficient excluding pure water at 710 nm $[a_{t-w}(710)]$ and the waveband ratio $r_{rs}(710)/r_{rs}(560)$.

Performing a Levenberg–Marquardt regression analysis on the Poyang Lake simulated data, empirical parameters in Table 2 of Lee et al.[6] were reset as follows: $T \approx 0.53$, $\kappa \approx 1.74$, $g_0 \approx 0.09$, and $g_1 \approx 0.12$. These regression results are similar to the original values[6] ($T \approx 0.52$, $\kappa \approx 1.7$, $g_0 \approx 0.09$, and $g_1 \approx 0.13$). Due to the high-suspended sediment concentration in Poyang Lake, the pure water backscattering coefficient can be neglected when calculating $b_{bp}(710)$. So, the $a_{t-w}(710)$ and $b_{bp}(710)$ can be calculated as follows in Fig. 3(a):

$$a_{t-w}(710) = 0.120 + 0.665\left(\frac{r_{rs}(710)}{r_{rs}(560)}\right)^{4.298}, \tag{9}$$

$$b_{bp}(710) = \frac{u(710)a(710)}{1-u(710)}, \tag{10}$$

where $u(\lambda) = b_b(\lambda)/[b_b(\lambda) + a(\lambda)]$.

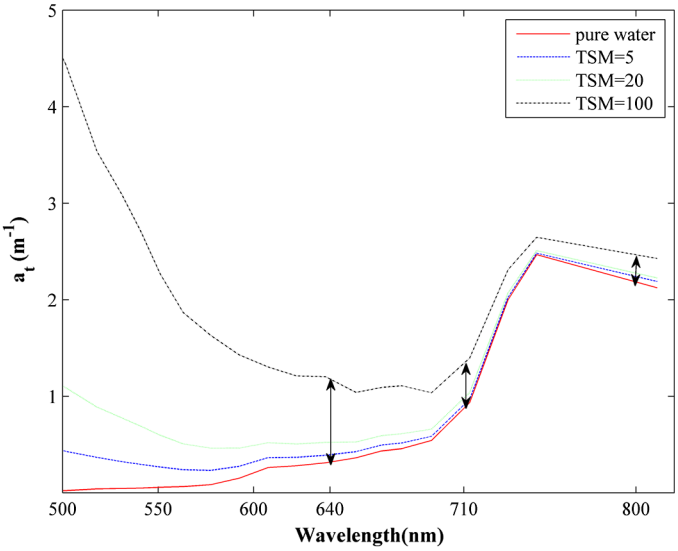

Fig. 2 Examples of a_t variations at different wavelengths.

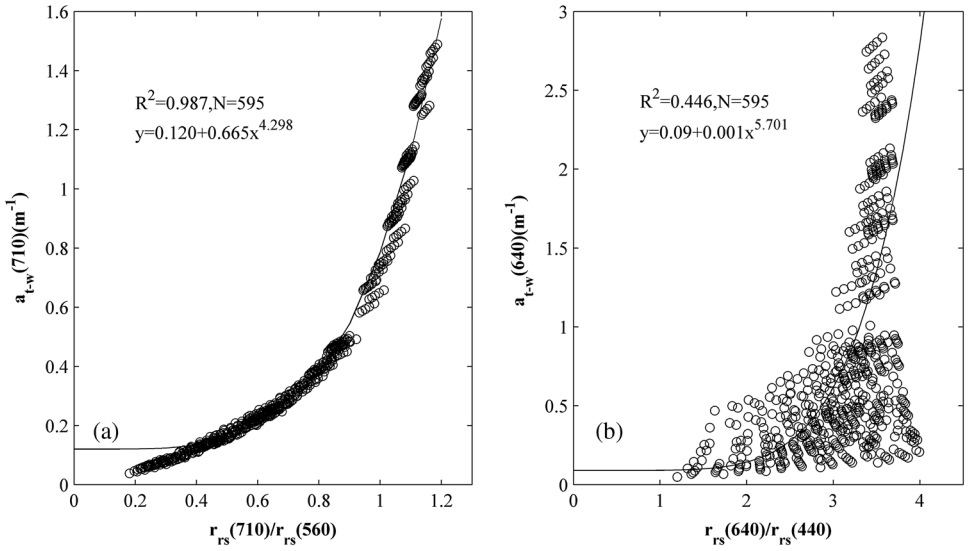

Fig. 3 New empirical models of the $a_{t-w}(\lambda)$, (a) QAA710 and (b) mQAA640.

The $b_{bp}(\lambda)$ varies in a power-law function of wavelength. Through iteration of simulated data, the spectral slope of $b_{bp}(\lambda)$ (Y) at 710 nm was found to be 0.862.

$$b_{bp}(\lambda) = b_{bp}(710)\left(\frac{710}{\lambda}\right)^{0.862}. \tag{11}$$

To validate the QAA710 model [see Fig. 3(a) and Eqs. (9)–(11)] comprehensively, we also modified the original QAA model with simulated data. Through a similar process, a modified QAA640 model (mQAA640) was built with new empirical parameters and formulas [see Fig. 3(b) and Eqs. (12)–(14)].

$$a_{t-w}(640) = 0.09 + 0.001\left[\frac{r_{rs}(640)}{r_{rs}(440)}\right]^{5.701}, \tag{12}$$

$$b_{bp}(640) = \frac{u(640)a(640)}{1-u(640)} - b_{bw}(640), \tag{13}$$

$$b_{bp}(\lambda) = b_{bp}(640)\left(\frac{640}{\lambda}\right)^{0.784}. \tag{14}$$

3.3 *Assessment of the Derived Products*

To assess the performance of the retrieval models, the mean relative errors (MRE) and the coefficient of determination (R^2) are commonly used. Because the derived IOPs are often considered to bear a log-normal distribution,[34] the root mean square errors in $\log_{10}$ scale (log-RMSE) and the linear percentage error (ε) were also calculated. These parameters are defined as follows:

$$\mathrm{MRE} = \left(\frac{1}{N}\sum_{i=1}^{N}\frac{a_i^{mea} - a_i^{est}}{a_i^{mea}}\right) \times 100\%, \tag{15}$$

$$\log\text{-RMSE} = \left\{\frac{1}{N}\sum_{i=1}^{N}[\log(a_i^{mea}) - \log(a_i^{est})]^2\right\}^{1/2}, \tag{16}$$

$$\varepsilon = (10^{\log - \mathrm{RMSE}} - 1) \times 100\%, \tag{17}$$

where a_i^{est} stands for the i'th property derived from $R_{\mathrm{rs}}(\lambda)$, a_i^{mea} stands for the i'th property obtained from *in situ* data, and N is the number of retrievals.

4 Results

4.1 *Simulated Data Sets*

As described in Sec. 3, we simulated 850 data sets with Hydrolight model.

Two representative observation sites (labeled with stars in Fig. 1) with different water qualities and geographical conditions are selected for comparison. Observation site PY2008 is located at the southern end of the waterway near the tributaries confluence, which is characterized by complex hydrologic features. The TSM, Chl, and CDOM at PY2008 are 104.8 mg/l, 7.19 μg/l, and 0.44 m^{-1}, respectively. Observation site PY2104 is situated near the center of the main lake, with relatively clear water. The TSM, Chl, and CDOM at PY2104 are 6.02 mg/l, 4.39 μg/l, and 1.63 m^{-1}, respectively. As discussed in Sec. 3.2, the waveband ratio $r_{\mathrm{rs}}(710)/r_{\mathrm{rs}}(560)$ was used in the QAA710 model; thus, the R_{rs} spectra were normalized to 560 nm. In Fig. 4, the simulated R_{rs} spectra share a similar trend with the measured spectra. The ε at 440, 550, 640, and 710 nm are 4.9%, 0.1%, 0.3%, and 0.6%, respectively. Similar results are observed at other sites. This comparison demonstrates that spectral shapes of the simulation agree well with measurements.

4.2 *Model Comparison with Simulated Data*

4.2.1 *Total absorption coefficient*

The QAA710-derived $a_{\mathrm{t}}(\lambda)$ and mQAA640-derived $a_{\mathrm{t}}(\lambda)$ are compared with the corresponding simulated data. Results at 440, 550, 640, and 710 nm are examined in Figs. 5 and 6. The derived $a_{\mathrm{t}}(\lambda)$ of the mQAA640 model significantly deviate from the 1:1 line for all four bands. The deviation enlarges along with wavelength. The mQAA640 model overestimates the $a_{\mathrm{t}}(\lambda)$ in the low-value sector but underestimates the $a_{\mathrm{t}}(\lambda)$ in the high-value sector, leading to large errors. The MRE ranges from −32.2% to −49.6% and ε ranges from 13.6% to 16.1%, showing obvious

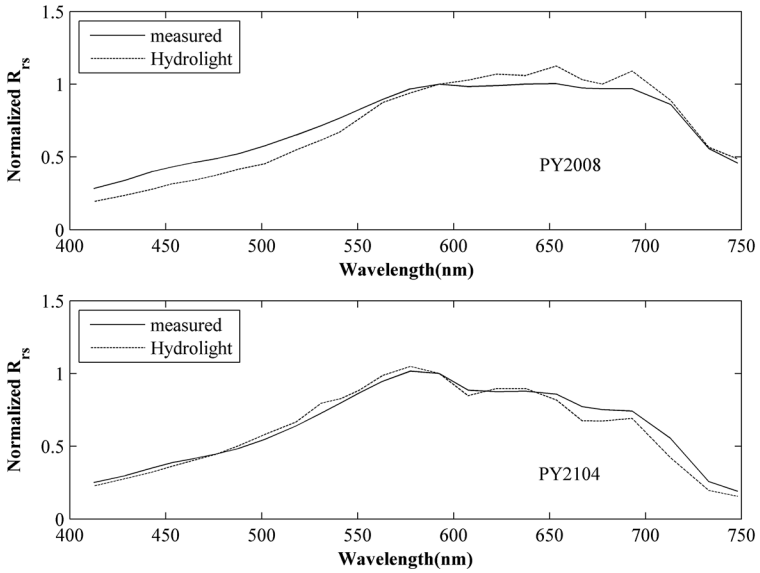

Fig. 4 Comparison of normalized hydrolight simulated R_{rs} and field-measured R_{rs} at observation sites PY2008 and PY2104 (labeled with stars in Fig. 1).

overestimation for four bands. In contrast, the derived $a_t(\lambda)$ from QAA710 shows a good correlation with the simulated data, with R^2 over 0.9 and an intercept value <0.2. The inversion accuracy at 710 nm surpasses the other three wavebands with a MRE of −0.2% and ε of 0.04%, followed by 640 nm (MRE 4.2% and ε 0.1%) and 440 nm (MRE −5.2% and ε 0.2%). The MRE of the QAA710 model at 550 nm is 7.7%, signifying a slight underestimation. This analysis demonstrates that the QAA710 model obviously surpasses the mQAA640 model. QAA710 performs quite well at the low and middle ranges of $a_t(\lambda)$, but produces relatively larger errors in the high-value sector for all four wavebands.

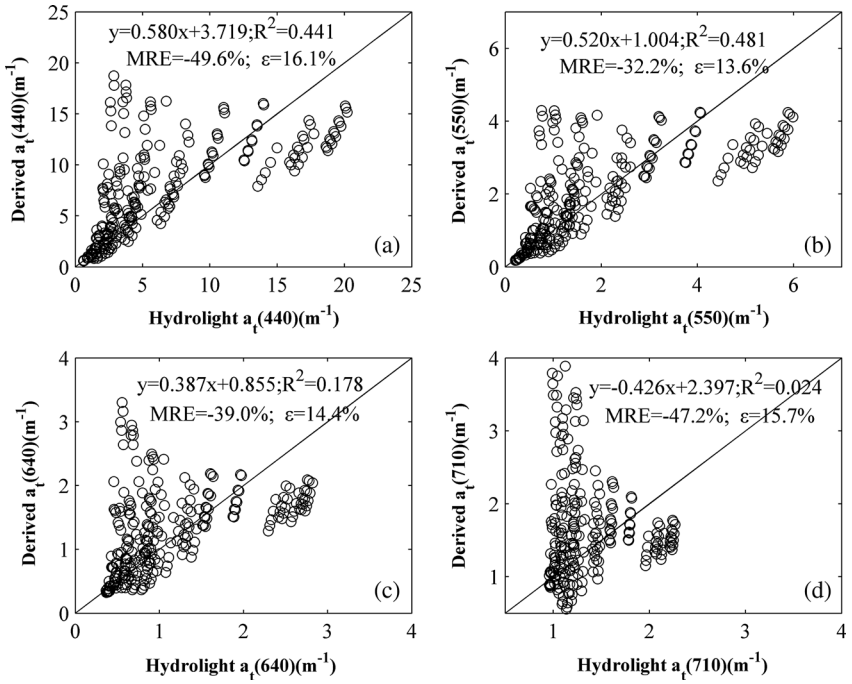

Fig. 5 Comparison of the $a_t(\lambda)$ inverted by the mQAA640 model versus simulated data.

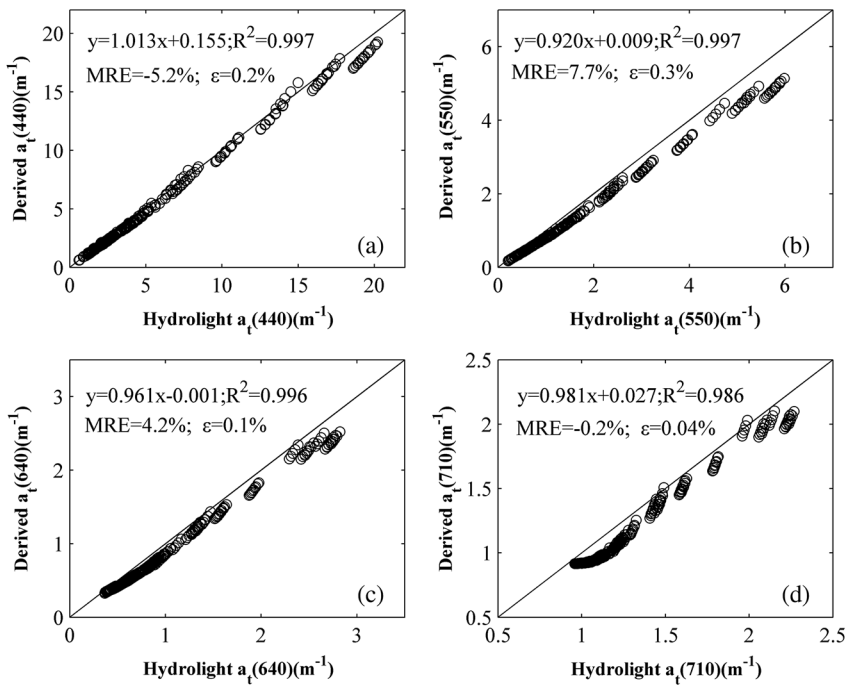

Fig. 6 Comparison of the $a_t(\lambda)$ inverted by the QAA710 model versus simulated data.

Figure 7 shows the worst and best case for the derived $a_t(\lambda)$. The TSM in Figs. 7(a) and 7(b) are 80 and 150 mg/l, the Chl are 15 and 1.5 μg/l, and the CDOM are 2.0 and 1.5 m^{-1}, respectively. The two inversion results are close to one another throughout the entire waveband in Fig. 7(a). Both the QAA710 model and mQAA640 model overestimate $a_t(\lambda)$, particularly in the violet–blue waveband, with a MRE of 8.9% and 13.7%, respectively. Slight overestimations can be observed around 750 nm for both models. Further analysis reveals that the QAA710-derived $a_t(\lambda)$ is 11.7% higher than the simulated $a_t(\lambda)$ in the violet–blue waveband (410 to 500 nm) but only 5.6% higher than the simulated $a_t(\lambda)$ in longer wavelengths (600 to 710 nm). Figure 7(b) illustrates the best case for the QAA710 model with a MRE of 4.2%, whereas the mQAA640 model overestimates $a_t(\lambda)$ with a MRE of 21.2%. Similarly, both models yield larger errors for violet–blue wavebands.

4.2.2 *Particulate backscattering coefficient*

The patterns of the derived $b_{bp}(\lambda)$ in Figs. 8 and 9 are similar to $a_t(\lambda)$ (Figs. 5 and 6). The mQAA640 model overestimates $b_{bp}(\lambda)$ in the low-value sector and underestimates $b_{bp}(\lambda)$ in the high-value sector with the biggest deviation at 710 nm. In general, the mQAA640 model overvalues $b_{bp}(\lambda)$ and MRE values range from −44.3% to −58.5%. In contrast, the scatter plot of the QAA710 model mostly conforms to the 1:1 line, returning MRE values between −2.0% and −12.8%, ε between 1.0% and 1.5% and R^2 over 0.99. The inversion accuracy at 550 nm surpasses the other three wavebands with a MRE of −2.0% and ε of 1.0% while 440 nm gets the largest deviation with a MRE of −12.8% and ε of 1.5%. Similarly, the QAA710 model yields bigger errors at high-value sector than low-value sector for $b_{bp}(\lambda)$.

4.3 *Model Comparison with Simulated Data Containing Random Noise*

In Sec. 4.2, the QAA710 model is validated with error-free simulated data. However, in the real world, measured data will not as good as above because of the measurement process, imperfect sensor calibration or atmospheric correction. To evaluate the QAA710 model with erroneous data, test 1 and test 2 introduced ±5% to ±20% random noise into the simulated r_{rs}. Green–blue wavelengths usually return larger errors than the red-infrared waveband in an atmospheric correction and IOPs retrieval. Thus, test 1 added ±5% random noise to the simulated $r_{rs}(640)$ and $r_{rs}(710)$, and ±10% random noise was added to the simulated r_{rs} at 440 and

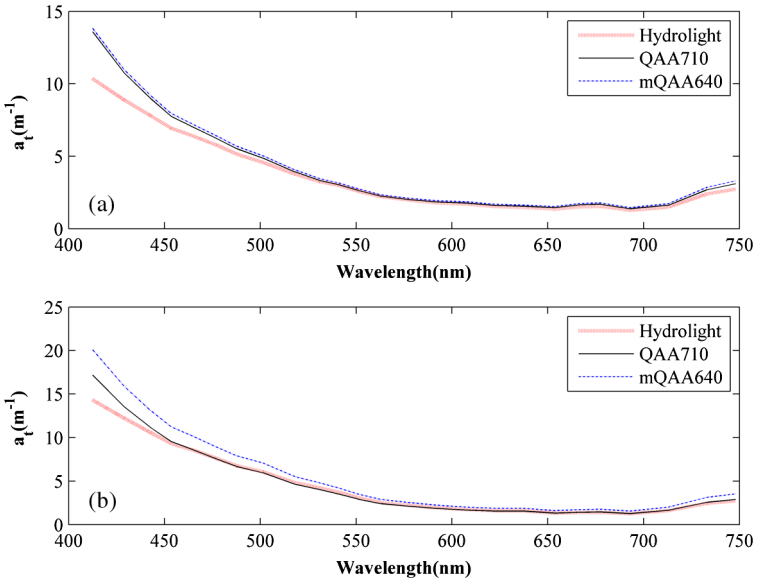

Fig. 7 Comparison of the worst (a) and best (b) inverted $a_t(\lambda)$ by the QAA710 model, mQAA640 model versus simulated data.

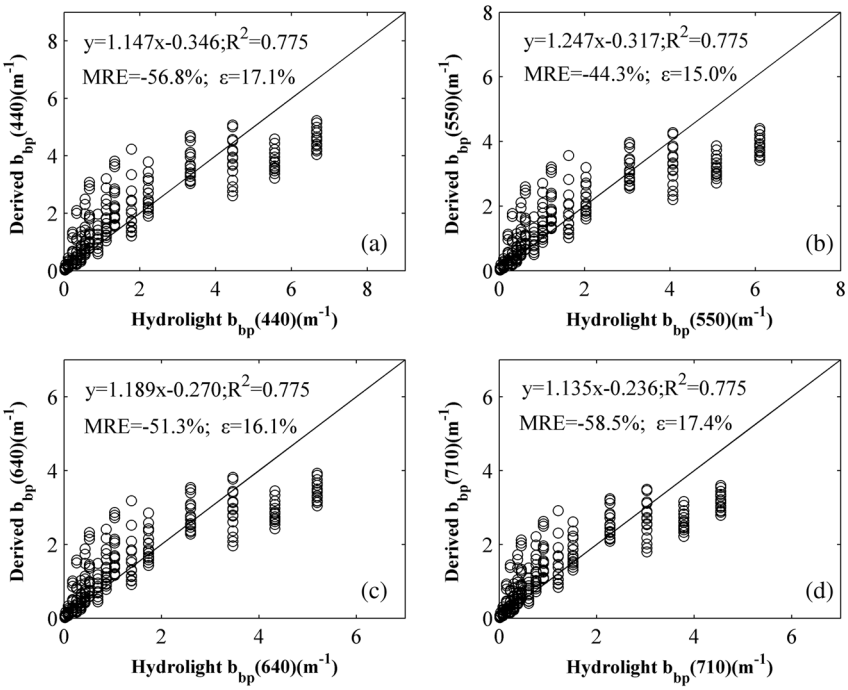

Fig. 8 Comparison of the $b_{bp}(\lambda)$ inverted by the mQAA640 model versus simulated data.

550 nm. In test 2, ±10% random noise was added to $r_{rs}(640)$ and $r_{rs}(710)$, and ±20% random noise was added to $r_{rs}(440)$ and $r_{rs}(550)$.

Figures 10(a) and 10(c) show the derived results with ±5% and ±10% random noise added to the $r_{rs}(550)$ and $r_{rs}(640)$, respectively. Although the r_{rs} values contain random noise, the QAA710 model still returns satisfying derived $a_t(\lambda)$ (band-averaged MRE 4.3%, ε 0.5%, R^2 0.941) and $b_{bp}(\lambda)$ (band-averaged MRE 7.3%, ε 1.6%, R^2 0.960). Not surprisingly, larger random noises (±10% and ±20%) exert greater influences on the derived $b_{bp}(\lambda)$ than $a_t(\lambda)$, as

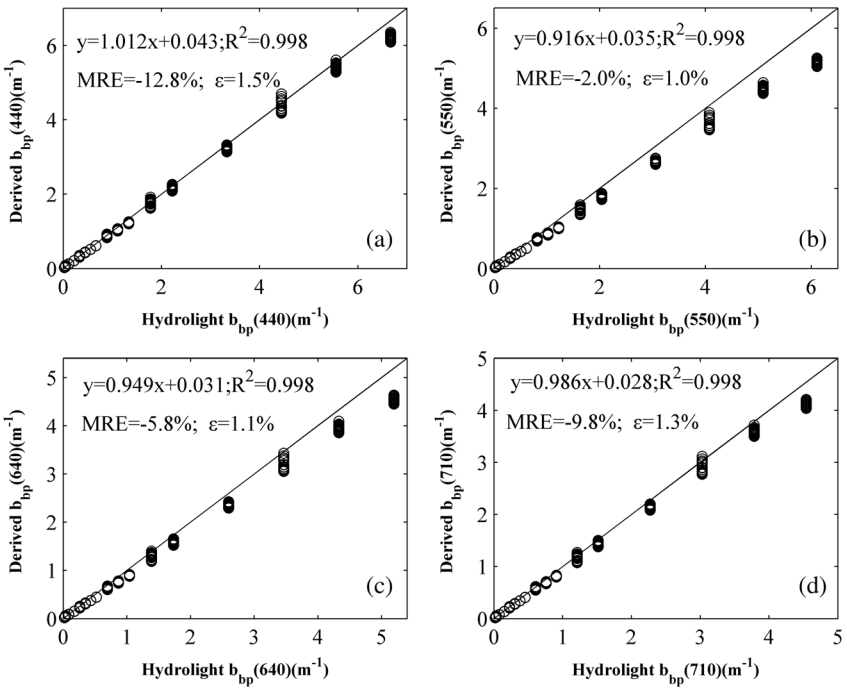

Fig. 9 Comparison of the $b_{bp}(\lambda)$ inverted by the QAA710 model versus simulated data.

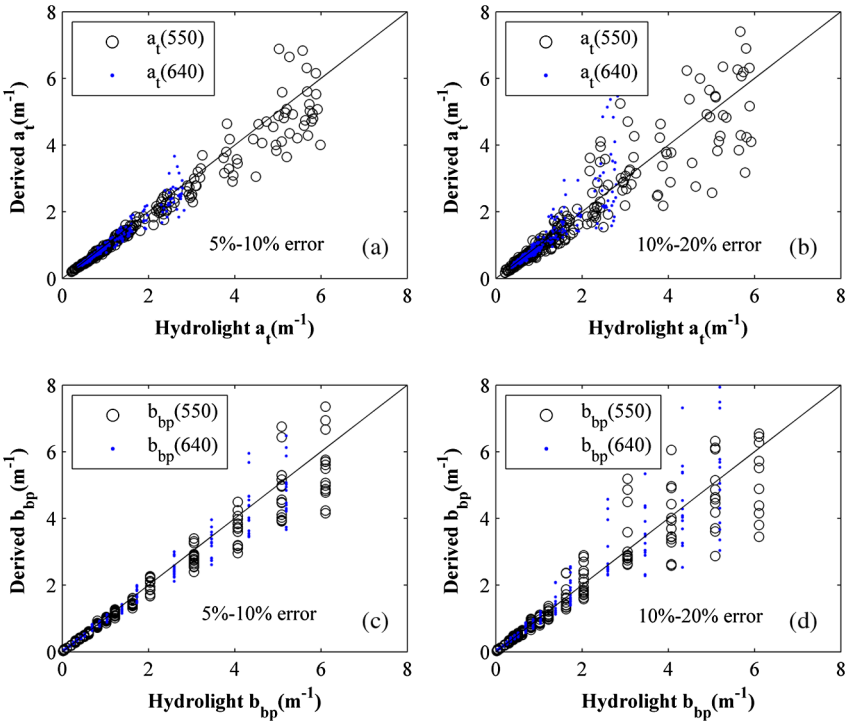

Fig. 10 Comparison of the QAA710-derived $a_t(\lambda)$ (a, b) and $b_{bp}(\lambda)$ (c, d) versus simulated data after 5% to 10% (a, c) and 10% to 20% (b, d) random noise were added to the r_{rs}.

shown in Figs. 10(b) and 10(d). The band-averaged MRE for $a_t(\lambda)$ is 4.1% but 12.0% for $b_{bp}(\lambda)$. In summary, the QAA710 model is quite noise tolerant, at least for the $a_t(\lambda)$ retrieval.

It should be noted that the validations shown in Secs. 4.2 and 4.3 with the simulated data only provide a general performance description of the QAA710 model. This is because simulated data from radiative transfer simulation still cannot represent the diversity in natural water. In addition,

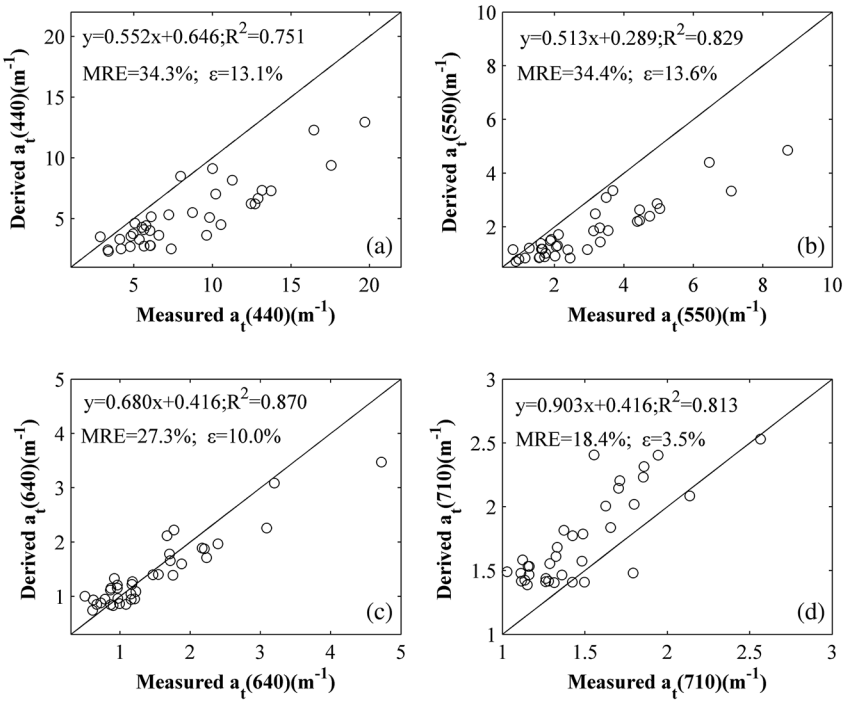

Fig. 11 Comparison of the QAA710-derived $a_t(\lambda)$ versus field-measured $a_t(\lambda)$ at four wavebands.

the empirical Eqs. (9)–(11) may not accurately describe the actual responses of optical properties to biogeochemical processes. Therefore, field-measured data must be used to validate the QAA710 model.

4.4 *Validation of the QAA710 Model with In Situ Data*

Because of the high turbidity of Poyang Lake and the limited measuring range of optical equipment, no valid $b_{bp}(\lambda)$ was acquired for comparison. Only 37 sets of field measured $a_t(\lambda)$ (see Table 1) were used to validate the QAA710 model.

The derived $a_t(\lambda)$ show a good correlation with the measured data, with the R^2 over 0.75 for four bands (Fig. 11). Further statistical analysis reveals larger discrepancies at 440 and 550 nm (MRE ~34%, $\varepsilon \sim 13\%$) than at the other two wavelengths. Most points in the scatter plot at 640 and 710 nm lie close to the 1 : 1 line and return smaller errors (MRE 27.3% and 18.4%, ε 10.0% and 3.5%, respectively). The inversion accuracy at 710 nm surpasses the other three wavebands while 550 nm returns the largest deviation. The band-averaged MRE of 28.6% and ε of 10.0% demonstrates that the QAA710 model performs well with *in situ* data. Similar to the validation with simulated data, the QAA710 model yields better results at the red-infrared waveband than at the violet–blue waveband with relatively larger deviation at the higher-absorbing end.

5 Discussion

This research generated a set of simulated data to make up for the deficiency of *in situ* data and modified the QAA model by switching the reference wavelength to 710 nm, resulting in better derived results for IOPs in highly turbid Poyang Lake. Choosing a suitable reference wavelength is crucial for a successful retrieval. Figure 2 demonstrates that the absorption at 555 or 640 nm is dominated by suspended solids in turbid Poyang Lake. As a result, the reference wavelength should be shifted to 710 nm. This reference wavelength not only guarantees the accurate estimation of a_t, but also makes the modified model appropriate for satellite images. 710 nm was first adopted by Doron et al.[14] in modeling, and then used by Le et al.[15] and Qing et al.[5] in their models for Taihu Lake and coastal Yellow and East China Sea. These successful retrievals certify the good adaptability of this reference wavelength in different turbid waters.

There are some sources of error of QAA710 model. First, the Hydrolight simulation inevitably introduces uncertainties. The QAA710 model was built with Hydrolight simulated data, which supplement the water optical properties of Poyang Lake. The Hydrolight is computationally efficient with no statistical uncertainty, but it simplifies the radiative transfer equations based on some assumptions. For example, the dredging activities around the Songmen Mountain severely disturb the water environment, causing the resuspension of sediment and extremely high turbidity. Thus, the scattering of particles near the water surface may contribute to the air-water interface, which is beyond the consideration of a standard Hydrolight simulation. In addition, we assumed an indefinite depth in the simulation according to the survey. However, the bottom effect introduces uncertainties into the Hydrolight simulation for optical clear water.[26] So, the clear southern part of main lake may be influenced by bottom effects and stratification. These uncertainties in the IOPs or boundary conditions lead to correspondingly errors in the computed radiance, and then in the retrieval results.

Second, the modeling of QAA710 also produces uncertainties. Lee et al.,[35] developed analytical functions to illustrate and evaluate the uncertainties and their propagations of IOPs derived by the original version of QAA. The most likely uncertainty of QAA-derived $a(440)$ is about $\pm 37\%$ for $a(440)_{QAA}$ approaching 0.5 m^{-1}. Moreover, higher b_{bp} could cause larger uncertainty, resulting from error in b_{bp} extrapolation. Taking the high turbidity of Poyang Lake into consideration, the uncertainties of QAA710 (band averaged MRE 28.6%) is acceptable.

Another error source of the QAA710 model may lie in the characteristics of field-measured validation data. The field-measured data for validation inevitably contain uncertainties caused by the observation procedure, weather condition, equipment calibration, gas-water contact, and bottom effect, particularly in clear waters.[36] These uncertainties may enlarge the differences between the derived IOPs and the field-measured values.

6 Conclusion

This article modified and validated the QAA model for retrieving the IOPs in the highly turbid Poyang Lake. In order to compensate the incompleteness of the *in situ* data of Poyang Lake, a large set of simulated data was produced using the Hydrolight radiative transfer model. Then, the QAA model was modified with the simulated data by shifting the reference wavelength to 710 nm and setting new empirical parameters. This reference wavelength not only guarantees the accurate estimation of a_t, but also makes the new model applicable to satellite images such as MERIS. Compared with the original model, the QAA710 model worked better with error-free simulated data and simulated data with random noise. A band-averaged MRE value of 28.6% and a ε of 10.0% demonstrated that the QAA710 model also performed well with *in situ* data. Nevertheless, the modeling process and the characteristics of modeling data and validation data introduced uncertainties into QAA710. Therefore, more independent tests with field measurements are required to completely validate and improve the accuracy of the model in Poyang Lake. The QAA710 model may also be applied to other highly turbid waters.

Acknowledgments

This study was supported by National Natural Science Foundation of China (41331174, 41301366, 41101415, and 41001260), National 863 Key Project (2012AA12A304), and Major Science and Technology Program for Water Pollution Control and Treatment (2013ZX07105-005). We would like to thank ESA Dragon Project (ID 10557).

References

1. D. A. Siegel, S. Maritorena, and N. B. Nelson, "Global distribution and dynamics of colored dissolved and detrital organic materials," *J. Geophys. Res.* **107**, 3228–3241 (2002), http://dx.doi.org/10.1029/2001JC000965.
2. A. Bricaud et al., "Retrieval of pigment concentrations and size structure of algal populations from their absorption spectra using multilayered perceptrons," *Appl. Opt.* **46**, 1251–1260 (2007), http://dx.doi.org/10.1364/AO.46.001251.
3. J. Marra, C. C. Trees, and J. E. O'Reilly, "Phytoplankton pigment absorption: a strong predictor of primary productivity in the surface ocean," *Deep-Sea Res.* **54**, 155–163 (2007), http://dx.doi.org/10.1016/j.dsr.2006.12.001.
4. F. Mélin, G. Zibordi, and J.-F. Berthon, "Assessment of satellite ocean color products at a coastal site," *Remote Sens. Environ.* **110**, 192–215 (2007), http://dx.doi.org/10.1016/j.rse.2007.02.026.
5. S. Qing et al., "Retrieval of inherent optical properties of the Yellow Sea and East China Sea using a quasi-analytical algorithm," *Chin. J. Oceanol. Limnol.* **29**, 33–45 (2011), http://dx.doi.org/10.1007/s00343-011-9967-z.
6. Z. P. Lee, K. L. Carder, and R. A. Arnone, "Deriving inherent optical properties from water color: a multiband quasi-analytical algorithm for optically deep waters," *Appl. Opt.* **41**, 5755–5772 (2002), http://dx.doi.org/10.1364/AO.41.005755.
7. M. Chami and M. D. Platel, "Sensitivity of the retrieval of the inherent optical properties of marine particles in coastal waters to the directional variations and the polarization of the reflectance," *J. Geophys. Res.* **112**, C05037 (2007), http://dx.doi.org/10.1029/2006JC003758.
8. T. W. Cui et al., "Satellite retrieval of inherent optical properties in the turbid waters of the Yellow Sea and the East China Sea," *Chin. Opt. Lett.* **8**, 721–725 (2010), http://dx.doi.org/10.3788/COL.
9. IOCCG, "Remote sensing of inherent optical properties: Fundamentals, tests of algorithms, and applications," in *International Ocean Colour Coordinating Group*, report number 5, Z. P. Lee, Ed. (2006).
10. S. Maritorena, D. A. Siegel, and A. R. Peterson, "Optimization of a semianalytical ocean color model for global-scale applications," *Appl. Opt.* **41**, 2705–2714 (2002), http://dx.doi.org/10.1364/AO.41.002705.

11. K. L. Carder et al., "Performance of the MODIS semi-analytical ocean color algorithm for chlorophyll-a," *Adv. Space Res.* **33**, 1152–1159 (2004), http://dx.doi.org/10.1016/S0273-1177(03)00365-X.
12. Z. P. Lee et al., "Euphotic zone depth: its derivation and implication to ocean-color remote sensing (QAA-V4)," *J. Geophys. Res.* **112**, C03009 (2007), http://dx.doi.org/10.1029/2006JC003802.
13. Z. P. Lee et al., "An update of the quasi-analytical algorithm (QAA_v5)," http://www.ioccg.org/groups/Software_OCA/QAA_v5.pdf (2009).
14. M. Doron et al., "Estimation of light penetration, and horizontal and vertical visibility in oceanic and coastal waters from surface reflectance," *J. Geophys. Res.: Oceans* **112**, C06003 (2007), http://dx.doi.org/10.1029/2006JC004007.
15. C. F. Le et al., "Validation of a quasi-analytical algorithm for highly turbid eutrophic water of Meiliang Bay in Taihu Lake, China," *IEEE Trans. Geosci. Remote Sens.* **47**, 2492–2500 (2009), http://dx.doi.org/10.1109/TGRS.2009.2015658.
16. J. Huang et al., "Validation of semi-analytical inversion models for inherent optical properties from ocean color in coastal Yellow Sea and East China Sea," *J. Oceanogr.* **69**, 713–725 (2013), http://dx.doi.org/10.1007/s10872-013-0202-8.
17. X. Chen et al., "Inversion model for dynamic monitoring of suspended sediment: a case study of Poyang Lake," *Sci. Technol. Rev.* **25**, 19–22, In Chinese with an English abstract (2007).
18. Q. Liu and D. G. Rossiter, "Estimation on suspended sedimentation concentration of Poyang Lake using MODIS and hyperspectral data," *Remote Sens. Technol. Appl.* **23**, 7–12, In Chinese with an English abstract (2008).
19. G. F. Wu et al., "Absorption and backscattering coefficients and their relations to water constituents of Poyang Lake, China," *Appl. Opt.* **50**, 6358–6368 (2011), http://dx.doi.org/10.1364/AO.50.006358.
20. L. Feng et al., "MODIS observations of the bottom topography and its inter-annual variability of Poyang Lake," *Remote Sens. Environ.* **115**, 2729–2741 (2011), http://dx.doi.org/10.1016/j.rse.2011.06.013.
21. L. Feng et al., "Assessment of inundation changes of Poyang Lake using MODIS observations between 2000 and 2010," *Remote Sens. Environ.* **121**, 80–92 (2012a), http://dx.doi.org/10.1016/j.rse.2012.01.014.
22. L. Chen, "Remote sensing of suspended particulate matter concentration in Poyang Lake, based on radiative transfer theory," Doctoral Dissertation, [D] Wuhan Unviersity, Wuhan, In Chinese with an English abstract (2011).
23. L. Feng et al., "Human induced turbidity changes in Poyang Lake between 2000 and 2010: observations from MODIS," *J. Geophys. Res.* **117**, C07006 (2012b), http://dx.doi.org/10.1029/2011JD017012.
24. G. Huang, "On ecological security and ecological construction of Poyang Lake district," *Sci. Technol. Rev.* **24**, 73–78, In Chinese with an English abstract (2006).
25. M. Babin, D. Stramski, and G. M. Ferrari, "Variations in the light absorption coefficients of phytoplankton, nonalgal particles, and dissolved organic matter in coastal waters around Europe," *J. Geophy. Res.* **108**, 843–859 (2003), http://dx.doi.org/10.1029/2001JC000882.
26. B. Sundarabalan, P. Shanmugam, and S. Manjusha, "Radiative transfer modeling of upwelling light fields in coastal waters," *J. Quant. Spectrosc. Radiat. Transf.* **121**, 30–44 (2013), http://dx.doi.org/10.1016/j.jqsrt.2013.01.016.
27. Z. P. Lee et al., "An inherent-optical-property-centered approach to correct the angular effects in water-leaving radiance," *Appl. Opt.* **50**, 3155–3167 (2011), http://dx.doi.org/10.1364/AO.50.003155.
28. R. Pope and E. Fry, "Absorption spectrum (380–700 nm) of pure waters: II. Integrating cavity measurements," *Appl. Opt.* **36**, 8710–8723 (1997), http://dx.doi.org/10.1364/AO.36.008710.
29. C. S. Roesler and M. J. Perry, "In situ phytoplankton absorption, fluorescence emission, and particulate backscattering spectra determined from reflectance," *J. Geophys. Res.* **100**, 13279–13294 (1995), http://dx.doi.org/10.1029/95JC00455.
30. R. W. Gould, R. A. Arnone, and P. M. Martinolich, "Spectral dependence of the scattering coefficient in case 1 and case 2 waters," *Appl. Opt.* **38**, 2377–2397 (1999), http://dx.doi.org/10.1364/AO.38.002377.

31. E. Aas, J. Høkedal, and K. Sørensen, "Spectral backscattering coefficient in coastal waters," *Int. J. Remote Sens.* **26**, 331–343 (2005), http://dx.doi.org/10.1080/01431160410001720324.
32. J. T. O. Kirk, "The vertical attenuation of irradiance as a function of the optical properties of the water," *Limnol. Oceanogr.* **48**, 9–17 (2003), http://dx.doi.org/10.4319/lo.2003.48.1.0009.
33. D. Y. Sun et al., "Partitioning particulate scattering and absorption into contributions of phytoplankton and non-algal particles in winter in Lake Taihu (China)," *Hydrobiologia* **644**, 337–349 (2010), http://dx.doi.org/10.1007/s10750-010-0198-7.
34. G. Campbell et al., "Remote sensing of water quality in an Australian tropical freshwater impoundment using matrix inversion and MERIS images," *Remote Sens. Environ.* **115**, 2402–2414 (2011), http://dx.doi.org/10.1016/j.rse.2011.05.003.
35. Z. P. Lee et al., "Uncertainties of optical parameters and their propagations in an analytical ocean color inversion algorithm," *Appl. Opt.* **49**, 369–381 (2010), http://dx.doi.org/10.1364/AO.49.000369.
36. S. B. Hooker and S. Maritorena, "An evaluation of oceanographic radiometers and deployment methodologies," *J. Atmos. Oceanic Technol.* **17**, 811–830 (2000), http://dx.doi.org/10.1175/1520-0426(2000)017<0811:AEOORA>2.0.CO;2.

Jue Huang is a PhD candidate at the State Key Laboratory of Information Engineering in Survey, Mapping and Remote Sensing, Wuhan University, China, where she is majoring in ocean color remote sensing. She is the author of three peer-reviewed papers and one book chapter.

Liqiong Chen got her PhD from State Key Laboratory of Information Engineering in Surveying, Mapping and Remote Sensing (LIESMARS), Wuhan University of China in 2011. She has worked as an engineer since 2012 at LIESMARS, Wuhan University, China. Her research interests are water color remote sensing and application of RS on water environment. She has published about 10 papers in English or Chinese.

Xiaoling Chen got her PhD from Department of Geography, Nanjing University of China in 1997. She worked as an associate professor from 1998 to 2000 and a professor since 2000 at the State Key Laboratory of Information Engineering in Surveying, Mapping and Remote Sensing (LIESMARS), Wuhan University, China. Her research interests are water/ocean color remote sensing and application of RS/GIS on ecology. She has published about 200 papers in English or Chinese.

Biographies for other authors are not available.